

¹ cosmo-numba: B-modes and COSEBIs computations accelerated by Numba

³ Axel Guinot  ¹ and Rachel Mandelbaum 

⁴ 1 Department of Physics, McWilliams Center for Cosmology and Astrophysics, Carnegie Mellon
⁵ University, Pittsburgh, PA 15213, USA

DOI: [10.xxxxxx/draft](https://doi.org/10.xxxxxx/draft)

Software

- ⁶ ▪ [Review](#) 
- ⁷ ▪ [Repository](#) 
- ⁸ ▪ [Archive](#) 

Editor: [Open Journals](#) 

Reviewers:

- ⁹ ▪ [@openjournals](#)

Submitted: 01 January 1970

Published: unpublished

License

¹⁵ Authors of papers retain copyright
and release the work under a
¹⁶ Creative Commons Attribution 4.0
¹⁷ International License ([CC BY 4.0](#))
¹⁸

Summary

⁷ Weak gravitational lensing is a widely used probe in cosmological analysis. It allows astrophysicists
⁸ to understand the content and evolution of the Universe. We are entering an era where we are
⁹ not limited by the data volume but by systematic uncertainties. It is in this context that we
¹⁰ present here a simple python-based software package to help in the computation of E-/B-mode
¹¹ decomposition, which can be used for systematic checks or science analysis. As we demonstrate,
¹² our implementation has both the high precision required and speed to perform this kind of
¹³ analysis while avoiding a scenario wherein either numerical precision or computational time is
¹⁴ a significant limiting factor.

Statement of need

¹⁵ The E-/B-mode composition for cosmic shear poses a significant computational challenge given
the need for high precision (required to integrate oscillatory functions over a large integration
range and achieve accurate results) and speed. Cosmo-numba meets this need, facilitating the
¹⁶ computation of E-/B-mode decomposition using two methods. One of them is the Complete
¹⁷ Orthogonal Sets of E-/B-mode Integrals (COSEBIs) as presented in P. Schneider et al. ([2010](#)).
¹⁸ The COSEBIs rely on very high precision computation requiring more than 80 decimal places.
¹⁹ P. Schneider et al. ([2010](#)) propose an implementation using mathematica. cosmo-numba uses
²⁰ a combination of sympy and mpmath to reach the required precision. This python version
²¹ enables an easier integration within cosmological inference pipelines, which are commonly
²² python-based, and facilitates the null tests.

²³ This software package also enables the computation of the pure-mode correlation functions
²⁴ presented in Peter Schneider et al. ([2022](#)). Those integrals are less numerically challenging than
²⁵ the COSEBIs, but having a fast computation is necessary for their integration in an inference
²⁶ pipeline. Indeed, one can use those correlation functions for cosmological inference, in which
²⁷ case the large number of calls to the likelihood function will require a fast implementation.

State of the field

³¹ There are other implementations of the COSEBIs such as CosmoPipe¹ used in the KiDS-legacy
³² analysis ([Wright et al., 2025](#)). Our implementation is characterized by the use of numba that
³³ makes the computation of the filter functions described in [section 6](#) faster. Regarding the
³⁴ pure E-/B-mode decomposition we have not found a similar publicly available implementation.
³⁵ That being said, they are classically used as a one time measure for null tests in various
³⁶ surveys. The implementation we are presenting would enable one to use this decomposition

¹ <https://github.com/AngusWright/CosmoPipe>

38 for cosmological inference that requires computing several integrals at each likelihood call.
 39 While commonly used library such as Scipy would make the computation untrackable, the
 40 speed gain by switching to numba open new perspectives such as this one.

41 Software design

42 This package has been designed around two constraints: precision and speed. As it can be
 43 difficult to reach both at the same time, the code is partitioned in a way that parts requiring
 44 high precision are done using python library such as sympy and mpmath. While parts of the
 45 code that do not require high precision leverage the power of Just-In-Time (JIT) compilation.
 46 Numba provides significant speed up compare to a classic python implementation. As this
 47 library is intended to provide tools from cosmological computation, it was important to provide
 48 meaningful unit tests and demonstrate a full coverage of the library. Providing an accurate
 49 coverage is challenging when using numba compiled code. Our implementation allows to disable
 50 compilation for targeted part of the code when performing coverage tests. This allows us to
 51 provide both high quality unit tests and good coverage to the users.

52 Testing setup

53 In the following two sections we make use of fiducial shear-shear correlation functions, $\xi_{\pm}(\theta)$,
 54 and power spectrum, $P_{E/B}(\ell)$. They have been computed using the Core Cosmology Library²
 55 ([Chisari et al., 2019](#)). The cosmological parameters are taken from Aghanim et al. ([2020](#)).
 56 For tests that involved covariance we are using the Stage-IV Legacy Survey of Space and
 57 Time (LSST) Year 10 as a reference. The characteristics are taken from the LSST Dark
 58 Energy Science Collaboration (DESC) Science Requirements Document (SRD) ([The LSST](#)
 59 [Dark Energy Science Collaboration et al., 2021](#)).

60 COSEBIs

61 The COSEBIs are defined as:

$$E_n = \frac{1}{2} \int_0^\infty d\theta \theta [T_{n,+}(\theta) \xi_+(\theta) + T_{n,-}(\theta) \xi_-(\theta)], \quad (1)$$

$$B_n = \frac{1}{2} \int_0^\infty d\theta \theta [T_{n,+}(\theta) \xi_+(\theta) - T_{n,-}(\theta) \xi_-(\theta)]; \quad (2)$$

63 where $\xi_{\pm}(\theta)$ are the shear correlation functions, and $T_{n,\pm}$ are the weight functions for the
 64 COSEBI mode n . The complexity is in the computation of the weight functions. Cosmo-numba
 65 carries out the computation of the weight functions in a logarithmic scale defined by:

$$T_{n,+}^{\log}(\theta) = t_{n,+}^{\log}(z) = N_n \sum_{j=0}^{n+1} \bar{c}_{nj} z^j; \quad (3)$$

66 where $z = \log(\theta/\theta_{\min})$, N_n is the normalization for the mode n , and \bar{c}_{jn} are defined iteratively
 67 from Bessel functions (we refer the readers to P. Schneider et al. ([2010](#)) for more details).

68 We have validating our implementation against the original version in Mathematica from P.
 69 Schneider et al. ([2010](#)). In [Figure 1](#) we show the impact of the precision going from 15 decimal
 70 places, which corresponds to the precision one could achieve using float64, up to 80 decimal
 71 places, the precision used in the original Mathematica implementation. We can see that classic

²<https://github.com/LSSTDESC/CCL>

72 float64 precision would not be sufficient, and with a precision of 80 our code exactly recovers
 73 the results from the original implementation. Given that the precision comes at very little
 74 computational cost, we default to the original implementation using high precision. The impact
 75 of the precision propagated to the COSEBIs is shown in Figure 2. We can see that using a
 76 lower precision than the default setting can incur a several percent error.

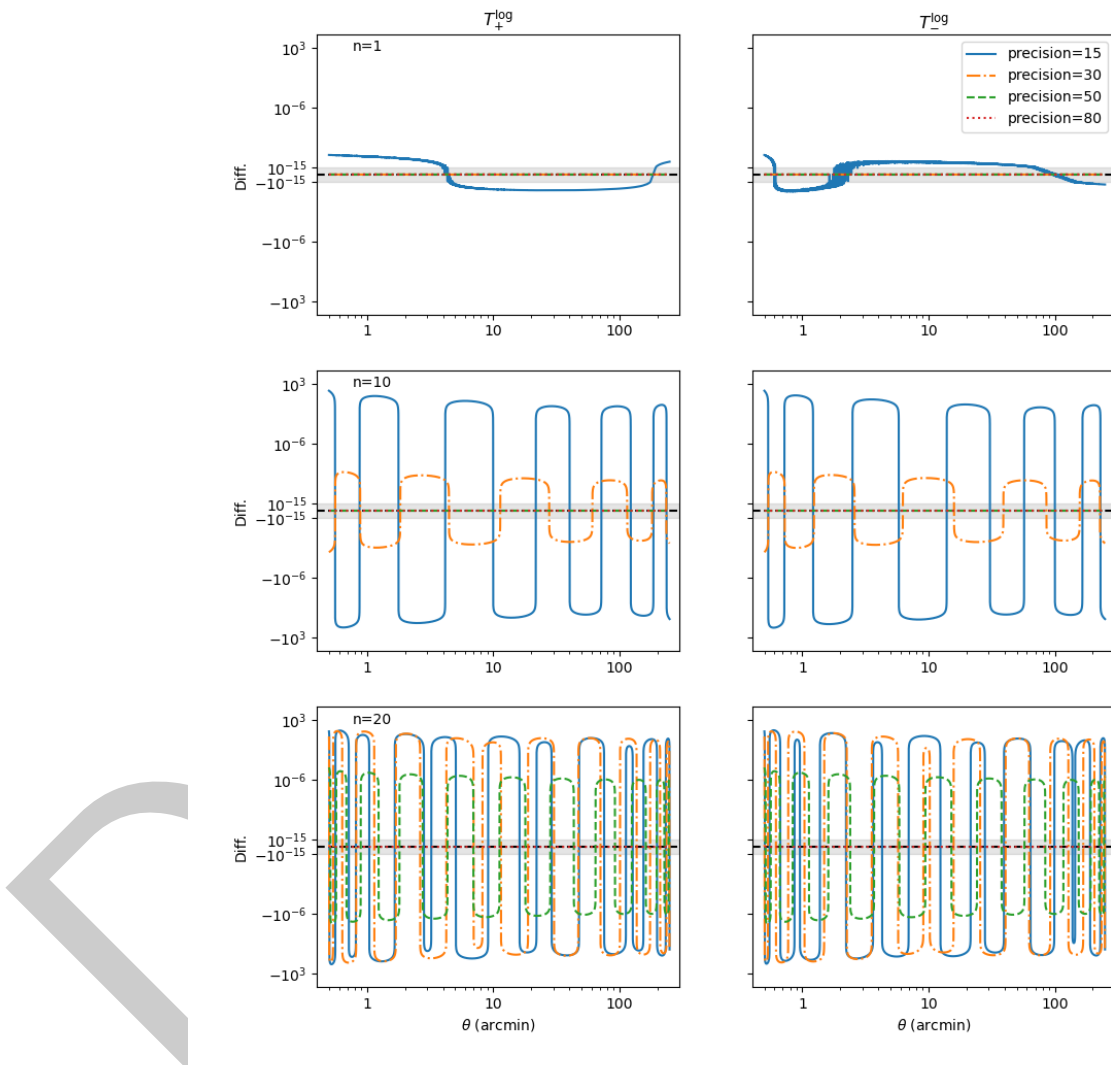


Figure 1: In this figure we show the impact of the precision in the computation of the weight functions T_{\pm}^{\log} . For comparison, a precision of 15 corresponds to what would be achieved using numpy float64. The difference is computed with respect to the original Mathematica implementation presented in P. Schneider et al. (2010). The figure uses symlog, with the shaded region representing the linear scale in the range $[-10^{-15}, 10^{-15}]$.

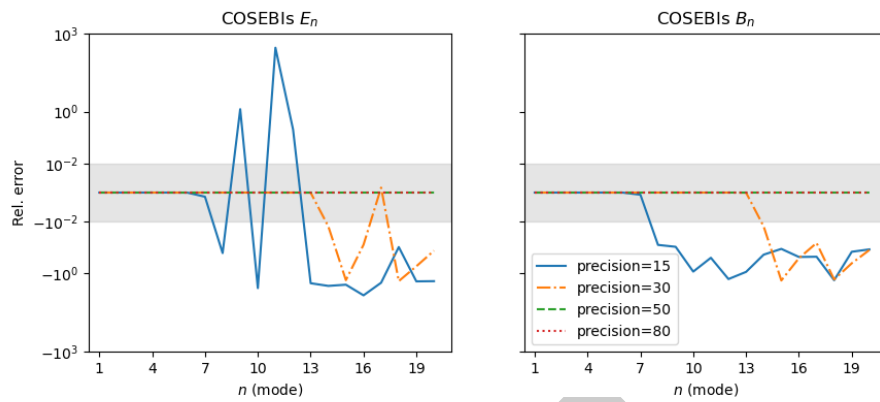


Figure 2: This figure shows the difference in the COSEBIs E- and B-modes relative to the original Mathematica implementation. We see that using only 15 decimal places would lead to several percent error, making an implementation based on numpy float64 not suitable. The figure uses symlog, with the shaded region representing the linear scale in the range $[-1, 1]$ percent.

⁷⁷ COSEBIs can also be defined from the power spectrum as:

$$E_n = \int_0^\infty \frac{d\ell \ell}{2\pi} P_E(\ell) W_n(\ell); \quad (4)$$

$$B_n = \int_0^\infty \frac{d\ell \ell}{2\pi} P_B(\ell) W_n(\ell); \quad (5)$$

⁷⁸ where $P_{E/B}(\ell)$ is the power spectrum of E- and B-modes and $W_n(\ell)$ are the filter functions
⁷⁹ which can be computed from $T_{n,+}$ as:

$$W_n(\ell) = \int_{\theta_{\min}}^{\theta_{\max}} d\theta \theta T_{n,+}(\theta) J_0(\ell\theta); \quad (6)$$

⁸⁰ with $J_0(\ell\theta)$ the 0-th order Bessel function. The [Equation 6](#) is a Hankel transform of order 0. It
⁸¹ can be computed using the FFTLog algorithm presented in [Hamilton \(2000\)](#) implemented here
⁸² in Numba. [Figure 3](#) shows the comparison between the COSEBIs computed from $\xi_{\pm}(\theta)$ and
⁸³ from $C_{E/B}(\ell)$. We can see that the COSEBI E- & B-modes agree very well, with at most 0.3σ
⁸⁴ difference with respect to the LSST Y10 covariance. We consider that using either approach
⁸⁵ would not impact the scientific interpretation and both could be used for consistency checks.
⁸⁶

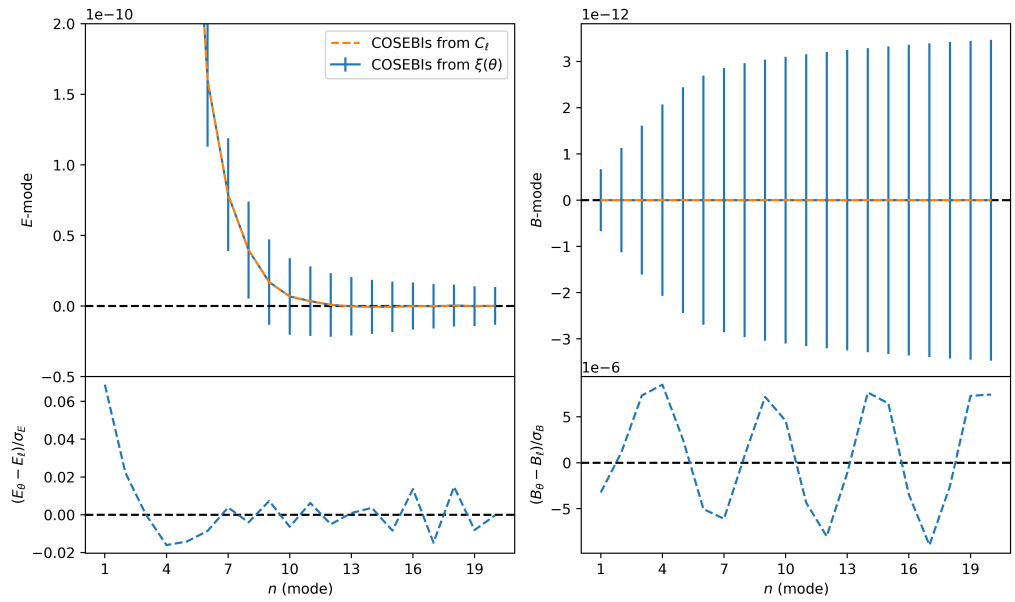


Figure 3: Comparison of the COSEBIs E- and B-mode computed from $\xi_{\pm}(\theta)$ and $C_{E/B}(\ell)$. The *upper* panel shows the COSEBIs E-/B-modes while the *bottom* panel shows the difference with respect to the statistical uncertainty based on the LSST Y10 covariance.

87 Pure-Mode Correlation Functions

88 In this section we describe the computation of the pure-mode correlation functions as defined
 89 in Peter Schneider et al. (2022). There are defined as follow:

$$\xi_+^E(\vartheta) = \frac{1}{2} \left[\xi_+(\vartheta) + \xi_-(\vartheta) + \int_{\vartheta}^{\vartheta_{\max}} \frac{d\theta}{\theta} \xi_-(\theta) \left(4 - \frac{12\vartheta^2}{\theta^2} \right) \right] - \frac{1}{2} [S_+(\vartheta) + S_-(\vartheta)], \quad (7)$$

$$\xi_+^B(\vartheta) = \frac{1}{2} \left[\xi_+(\vartheta) - \xi_-(\vartheta) - \int_{\vartheta}^{\vartheta_{\max}} \frac{d\theta}{\theta} \xi_-(\theta) \left(4 - \frac{12\vartheta^2}{\theta^2} \right) \right] - \frac{1}{2} [S_+(\vartheta) - S_-(\vartheta)], \quad (8)$$

$$\xi_-^E(\vartheta) = \frac{1}{2} \left[\xi_+(\vartheta) + \xi_-(\vartheta) + \int_{\vartheta_{\min}}^{\vartheta} \frac{d\theta \theta}{\vartheta^2} \xi_+(\theta) \left(4 - \frac{12\theta^2}{\vartheta^2} \right) \right] - \frac{1}{2} [V_+(\vartheta) + V_-(\vartheta)], \quad (9)$$

$$\xi_-^B(\vartheta) = \frac{1}{2} \left[\xi_+(\vartheta) - \xi_-(\vartheta) + \int_{\vartheta_{\min}}^{\vartheta} \frac{d\theta \theta}{\vartheta^2} \xi_+(\theta) \left(4 - \frac{12\theta^2}{\vartheta^2} \right) \right] - \frac{1}{2} [V_+(\vartheta) - V_-(\vartheta)]; \quad (10)$$

92 where $\xi_{\pm}(\theta)$ correspond to the shear-shear correlation function. The functions $S_{\pm}(\theta)$ and $V_{\pm}(\theta)$
 93 are themselves defined by integrals and we refer the reader to Peter Schneider et al. (2022)
 94 for more details about their definition. By contrast with the computation of the COSEBIs,
 95 these integrals are more stable and straightforward to compute but still require some level
 96 of precision. This is why we are using the qags method from QUADPACK³ (Piessens et al.,
 97 2012) with a 5th order spline interpolation. In addition, as one can see from the equations
 98 above, the implementation requires a loop over a range of ϑ values. This is why having a fast

³<https://github.com/LSSTDESC/CCL>

99 implementation will be required if one wants to use those correlation functions in cosmological
 100 inference. In Figure 4 we show the decomposition of the shear-shear correlation function into
 101 the E-/B-modes correlation functions and ambiguous mode.

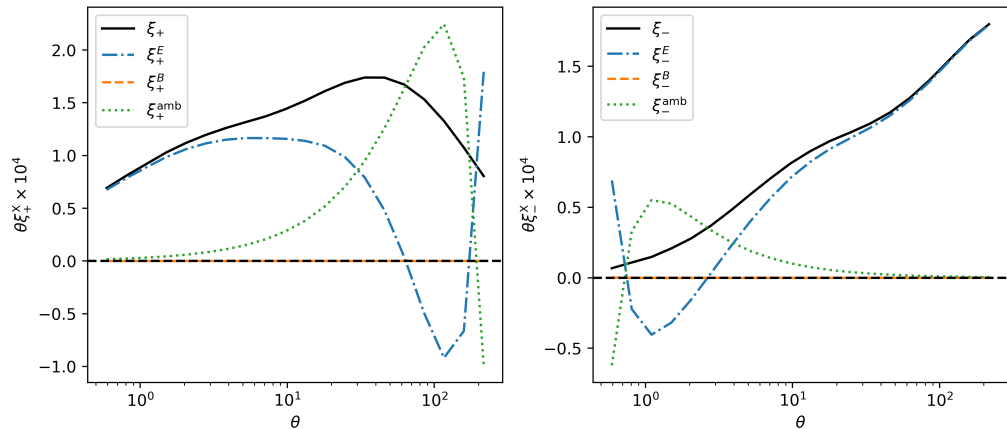


Figure 4: This figure shows the decomposition of the shear-shear correlation functions into E- and B-modes (and ambiguous mode).

102 Research impact statement

103 This software is being used in the Ultraviolet Near Infrared Optical Northern Survey (UNIONS) to
 104 validate the catalogue used for cosmological analysis (REF: Daley et al. 2026). We are also
 105 planning to use this code in the Roman High Latitude Imaging Survey (HLIS). In addition
 106 its current usage in science collaboration, we provide unit tests that not only validate the
 107 implementation but also validate the computation mathematically and provide a higher bound
 108 for the accuracy of the code. Finally, examples can be found in the code repo that provide
 109 comparison against alternative approach and implementation. They show that the computation
 110 presented here is significantly faster than existing alternatives.

111 AI usage disclosure

112 Artificial Intelligence (AI) has been used to help with documentation, docstrings and for some
 113 of the unit tests.

114 Acknowledgements

115 The authors acknowledge the support of a grant from the Simons Foundation (Simons
 116 Investigator in Astrophysics, Award ID 620789).

117 References

- 118 Aghanim, N., Akrami, Y., Ashdown, M., Aumont, J., Baccigalupi, C., Ballardini, M., Banday,
 119 A. J., Barreiro, R. B., Bartolo, N., Basak, S., Battye, R., Benabed, K., Bernard, J.-P.,
 120 Bersanelli, M., Bielewicz, P., Bock, J. J., Bond, J. R., Borrill, J., Bouchet, F. R., ...
 121 Zonca, A. (2020). Planck 2018 results: VI. Cosmological parameters. *Astronomy & Astrophysics*, 641, A6. <https://doi.org/10.1051/0004-6361/201833910>

- 123 Chisari, N. E., Alonso, D., Krause, E., Leonard, C. D., Bull, P., Neveu, J., Villarreal, A., Singh,
124 S., McClintock, T., Ellison, J., Du, Z., Zuntz, J., Mead, A., Joudaki, S., Lorenz, C. S.,
125 Tröster, T., Sanchez, J., Lanusse, F., Ishak, M., ... Wagoner, E. L. (2019). Core cosmology
126 library: Precision cosmological predictions for LSST. *The Astrophysical Journal Supplement
127 Series*, 242(1), 2. <https://doi.org/10.3847/1538-4365/ab1658>
- 128 Hamilton, A. J. S. (2000). Uncorrelated modes of the non-linear power spectrum. *Monthly
129 Notices of the Royal Astronomical Society*, 312(2), 257–284. [https://doi.org/10.1046/j.
130 1365-8711.2000.03071.x](https://doi.org/10.1046/j.
130 1365-8711.2000.03071.x)
- 131 Piessens, R., Doncker-Kapenga, E. de, Überhuber, C. W., & Kahaner, D. K. (2012). *Quadpack:
132 A subroutine package for automatic integration* (Vol. 1). Springer Science & Business
133 Media.
- 134 Schneider, Peter, Asgari, M., Jozani, Y. N., Dvornik, A., Giblin, B., Harnois-Déraps, J.,
135 Heymans, C., Hildebrandt, H., Hoekstra, H., Kuijken, K., Shan, H., Tröster, T., &
136 Wright, A. H. (2022). Pure-mode correlation functions for cosmic shear and application to
137 KiDS-1000. *Astronomy & Astrophysics*, 664, A77. [https://doi.org/10.1051/0004-6361/202142479](https://doi.org/10.1051/0004-
138 6361/202142479)
- 139 Schneider, P., Eifler, T., & Krause, E. (2010). COSEBIs: Extracting the full e-/b-mode
140 information from cosmic shear correlation functions. *Astronomy and Astrophysics*, 520,
141 A116. <https://doi.org/10.1051/0004-6361/201014235>
- 142 The LSST Dark Energy Science Collaboration, Mandelbaum, R., Eifler, T., Hložek, R., Collett,
143 T., Gawiser, E., Scolnic, D., Alonso, D., Awan, H., Biswas, R., Blazek, J., Burchat, P.,
144 Chisari, N. E., Dell'Antonio, I., Digel, S., Frieman, J., Goldstein, D. A., Hook, I., Ivezić,
145 Ž., ... Troxel, M. A. (2021). *The LSST dark energy science collaboration (DESC) science
146 requirements document*. <https://arxiv.org/abs/1809.01669>
- 147 Wright, A. H., Stölzner, B., Asgari, M., Bilicki, M., Giblin, B., Heymans, C., Hildebrandt, H.,
148 Hoekstra, H., Joachimi, B., Kuijken, K., Li, S.-S., Reischke, R., Wietersheim-Kramsta,
149 M. von, Yoon, M., Burger, P., Chisari, N. E., Jong, J. de, Dvornik, A., Georgiou, C.,
150 ... Zhang, Y.-H. (2025). KiDS-legacy: Cosmological constraints from cosmic shear with
151 the complete kilo-degree survey. *Astronomy & Astrophysics*, 703, A158. <https://doi.org/10.1051/0004-6361/202554908>